

**References:** Sudarsky, D., Burrows, A. and Hubeny, I. 2003, *Ap.J.* (May 10); Burrows, A., Sudarsky, D. and Lunine, J.I., 2003, *Ap.J.*, arXiv:astro-ph/0304226

(1) Statement of the problem

Over 100 planets orbiting stars other than the Sun have been discovered, the majority nearby and detected indirectly through the radial velocity (Doppler spectroscopic) technique. These objects range in mass from of order 0.1 to 10 Jupiter masses. (Because of the ambiguity in the orbit inclination relative to the Earth, the masses are lower limits in all but a handful of cases; a random distribution of inclinations would yield physical masses no more than twice the Doppler masses in 90% of the objects). Semi-major axes of the detected planets are distributed roughly uniformly from 0.04AU to 5 AU, though the completeness of the sample drops significantly beyond an AU or so. Eccentricities are distributed much like those of binary star systems, with circularity imposed on the closest objects by tidal interaction with the parent stars. In only one definite case, where the planet transits across the star as seen from the Earth, is the planetary radius determined, and it is roughly consistent with that of a hydrogen-helium (Jovian-type) planet thermally inflated by proximity to the parent star. By extension, then, the vast majority of the Doppler spectroscopic detections—if not all—are extrasolar giant planets (EGP's): bodies like Jupiter orbiting other stars.

The tenuous nature of the correspondence between Jupiter and EGP's is evident in the lack of direct detection, and indeed a Jupiter at 5 AU from a Sun-like star likely represents the practical mass/semi-major axis limit of the technique. But more profound questions are raised by the distributions of the orbital elements. Although predictions of giant planet migration, notably by D.N.C. Lin (UC Santa Cruz) and colleagues, appeared many years before the detection of EGP's, the potential implications for the semi-major axis distribution of giant planets was not explicitly realized. Post facto, however, the semi-major axis distribution of EGP's can be understood in terms of preferred formation of the giant planets at or beyond the "ice-line" (the region at which water ice condenses, hence raising the surface density of solids and decreasing accretion time) followed by inward migration. Such a model does not explain the eccentricity distribution, though it is not ruled out by the distribution.

Alternative to formation in preferred regions of the protoplanetary disk is the possibility that instabilities in massive disks could trigger giant planet formation at most semimajor axes, and that subsequent gravitational interactions in a dynamically "overfull" system would alter orbits and result in ejection of some EGP's. Formation times much shorter than the disk lifetime are possible in such a model, which provides an explanation for the eccentricity distribution. However, the larger abundance of Jovian mass (up to 10  $M_J$ , roughly) objects compared to more stellar T-dwarfs (or brown dwarfs; 10-80  $M_J$ ) does not arise naturally from this planet formation model.

We seek to understand the nature and formation mechanisms of EGP's, both for their own sake and as a guide to the commonality of situations like our solar system, in which the inner region is devoid of giant planets and hence dynamically available for rocky terrestrial planets.

## (2) Status of current understanding

There is a potential compositional discriminant between the two EGP formation models outlined above, namely the metallicity contrast between the planet and its parent star. A formation model that favors growth at and beyond the disk ice line is based on modeling the growth of giant planets in relatively quiescent, less-massive disks. Under such conditions significant addition of gas to make a giant planet does not occur until initial accretion of a rocky and icy core seeds the collapse of gas. As the gas is added additional solids from the surrounds fall into the growing giant planet until the final product has significantly higher metallicity than the parent star. The size of the rocky and icy seed core is not itself the crucial determinant of the final metallicity; more important is that the relatively quiescent growth enables the addition of large amounts of additional solids throughout the growth process. This model explains both the high metallicity of Jupiter and Saturn relative to the Sun as well as the distribution of heavy elements throughout the interior, not just in the core. Conversely, the disk instability model requires conditions such that addition of rocky and icy material in significant amounts to the rapidly-formed protoplanets is unlikely. Therefore such a model is not a promising one to explain Jupiter and Saturn (both of which create additional difficulties for the disk instability model, including how one forms a regular satellite system in the process). It is possible that many or all of the EGP's form by the disk instability model, that is, giant planets come in two different flavors distinguished by the formation mechanism. Those formed via the disk instability process would have metallicities similar to that of their parent stars, while EGP's formed by core formation and slow accretion should be significantly enriched.

Considerable experience in analyzing the spectra of substellar objects has been accumulated since 1995, when the first definitive brown dwarf was discovered. A well-quantified extension of the stellar spectral sequence below the M-dwarf range (to so-called L- and T-dwarfs has been possible largely as a consequence of ground-based surveys (2-MASS and Sloan). The bottom of the T-dwarf subclass lies at an effective temperature of 800 K, above the range of all EGP's except for the most massive, youngest, or most proximate to the parent star (figure 1). Distinguishing objects later than the T-dwarf sequence, which we shall call EGP's without prejudice regarding brown dwarf vs. planet formation mechanisms, are water and ammonia cloud formation, strength of methane absorption features, disappearance of the strong alkali metal features around 1 micron wavelength, reversal of the J-K color from a bluing to a reddening with decreasing effective temperature, and a precipitous drop in the flux shortward of 4 microns. This list applies to isolated EGP's. For bound EGP's close enough to the parent star that stellar photons dominate in the near-infrared, the precipitous drop in near-IR flux is replaced by an entirely reflected component, and some of the other indicators change as well (figure 2).

While the EGP realm represents unexplored terrain, the experience gained from Jupiter/Saturn, L- and T-dwarfs provides some confidence that we can predict fluxes vs. wavelength in the effective temperature *terra incognita* from 800K down through 130 K. Major uncertainties include the role of clouds in damping the strong infrared excess in the 5 micron region, and the effects of stratospheric emissions and day-night temperature differences on bound EGP's. Minor uncertainties concern the details of the line absorption coefficients for individual molecules used to build the gaseous molecular component of the model spectra. Nonetheless, armed with these models we can predict brightnesses and detectability of EGP's, and as well suggest that metallicities can be derived from moderate resolution (R=1000) spectra to provide a potential constrain on formation models.

In what follows all EGP's fluxes at Earth are for a standard distance of 10 parsecs.

### (3) Description of key measurements needed

- I. Detection and analysis of free-floating EGP's. Figures 3 and 4 illustrate that detection of a 1 M<sub>J</sub> EGP 100 million years old and a 5M<sub>J</sub> EGP 5 billion years old are possible with GSMT, but the latter is too faint for comprehensive spectroscopy; indeed, its detectability depends upon the excess flux in the 5 micron region. The young Jupiter mass object, on the other hand, may be analyzed spectroscopically at selected wavelengths. Younger or more massive objects, will of course be easier targets; these two examples represent part of the defining envelope of detectability/analyzability for isolated EGP's in the near-infrared.
  
- II. Detection and analysis of bound EGP's. For bound systems the crucial parameters determining detectability are the contrast ratio of the planet relative to the star, and the angular separation between the two. Either coronagraphy or interferometry are required to pull the light of the planet out from behind the glare of the parent star, along with large telescope aperture to minimize the angular extent of the bright fringes of the parent star. GSMT will feature a very large mirror diameter, which coupled with advanced coronagraphs on the telescope could enable detection of bound EGP's. Figure 5 plots the model contrast ratio of planet to star versus wavelength for the system 55 Cnc, in which two planets have been detected by the Doppler spectroscopic method. The closer planet, 55 Cnc b, is both warmer and more heavily irradiated than 55 Cnc d, and has contrast ratios generally between  $10^{-6}$  and  $10^{-4}$  in the near-infrared to mid-infrared. However, its angular separation from the star as seen from Earth is less than 0.01 arcseconds, making it an impractical candidate for coronagraphic or interferometric techniques. The contrast ratio for 55 Cnc d is everywhere less than  $10^{-7}$  except in the 5 micron peak and beyond 10 microns. Depending upon the sophistication of the coronagraphy, GSMT might be able to detect a spectral contrast of  $10^{-7}$  in the

5 micron part of the spectrum at the angular separation of 55 Cnc d, namely 0.45". Figure 6 shows that the absolute flux of 55 Cnc d, an object  $\geq 4$  Jupiter masses, exceeds the sensitivity limit for GSMT photometry. Thus, this planet is a candidate for direct detection, though not necessarily spectroscopy, by GSMT. A handful of the known EGP cohort fall into this detectable category, others will likely be discovered soon by Doppler spectroscopic techniques, and GSMT itself could search candidate stars at larger semi-major axes to make direct detection discoveries.

- III. Transits: A handful (1%) of indirectly detected EGP's should transit across the face of their parent star. These are more likely to be those in close orbits, for which direct observation is otherwise not possible, and hence careful transit studies with large telescopes will be important. From the dimming of the parent star's light as a function of wavelength, spectra revealing EGP atmospheric constituents could be detected, as for HD209458b using HST. GSMT is a ground-based telescope, but its enormous atmosphere coupled with good siting should make it at least as valuable a tool for deriving optical and near-IR atmospheric absorptions from transits as is HST.

#### (4) Comparison with JWST and SIRTf

GSMT will be the dominant facility for the detection and spectroscopy of isolated EGP's through the 5 micron wavelength region, with JWST doing a better job beyond 5 microns, roughly. The ability to detect spectral features across a wide range of wavelengths from the two facilities will give a better set of constraints on abundances, on the effects of clouds on a particular object, and (for R=1000 spectroscopy) the surface gravity. The detectability of EGP's increases dramatically in the infrared, which allows JWST to compensate for its smaller aperture relative to GSMT.

For bound systems, even though the contrast ratio is better beyond 5-10 microns than it is shortward, more sophisticated coronagraphy and the much smaller diffraction limit of GSMT compared with JWST will be key to detecting EGP's at typical separations around nearby stars of 0.5"-1". JWST may do better for EGP's in very loose orbits around nearby stars, equivalent to an arcsecond or more, provided that the planetary effective temperature is large enough to ensure detection of the thermal radiation.

Transit studies may not be easy with JWST for operational reasons, even though it is in principle the better of the two devices from the point of view of photometric accuracy because it is space-based. The issue of using ground-based telescopes to do high precision photometry (relative precision of  $10^{-4}$  is required to detect atmospheric features) is a complicated one, but well worth considering because of the unique contributions that could be made for the tight orbit EGP's.

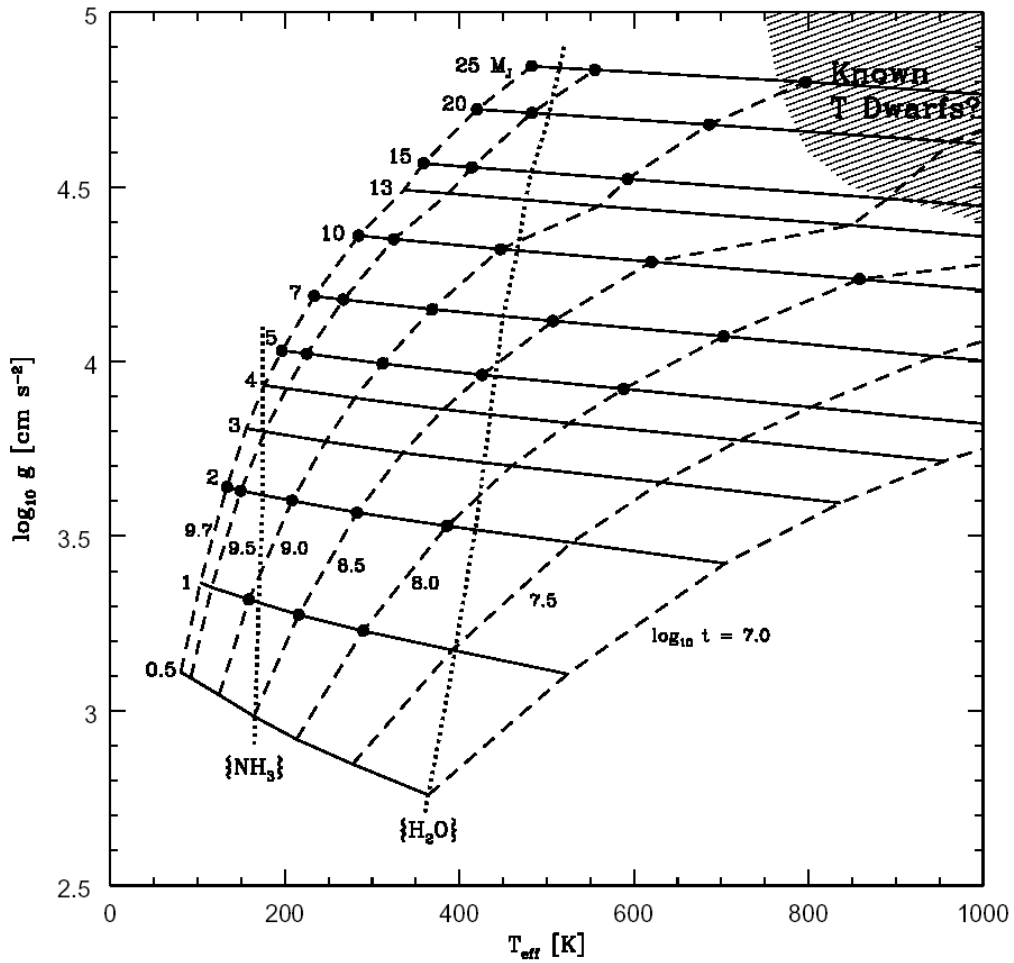


Figure 1. Surface gravity versus effective temperature (logarithmic) for isolated EGP's. Lines of constant mass and lines of constant age (logarithmic, years) define the grid for the solar composition objects modeled here. The realm of the coolest T-dwarfs occupies the upper right corner, with a minimum effective temperature of 740-800 K. Dashed lines demarcate the onset of water cloud and ammonia cloud formation near the unity optical depth level in the atmospheres. Bound EGP's will depart progressively from this grid according to the flux of energy they receive from their parent star. From Burrows et al. (2003).

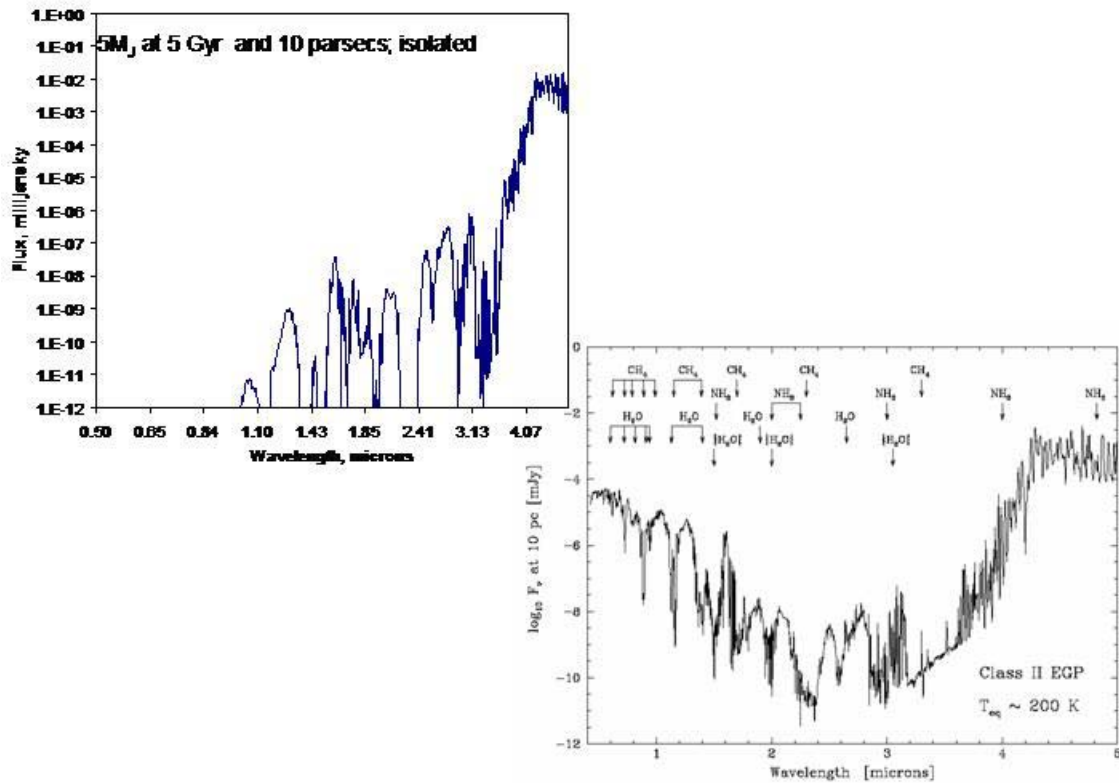


Figure 2. Comparison of EGP's with roughly the same effective temperature. Top model is an isolated object; bottom model is a bound EGP some 1-2AU from a solar-type star. Both plots are flux at Earth (millijansky) versus wavelength in microns. The reflected stellar light for the bound EGP fills in the flux in the region shortward of 2 microns. Models from Burrows et al. 2003 (top) and Sudarsky et al. 2003 (bottom).

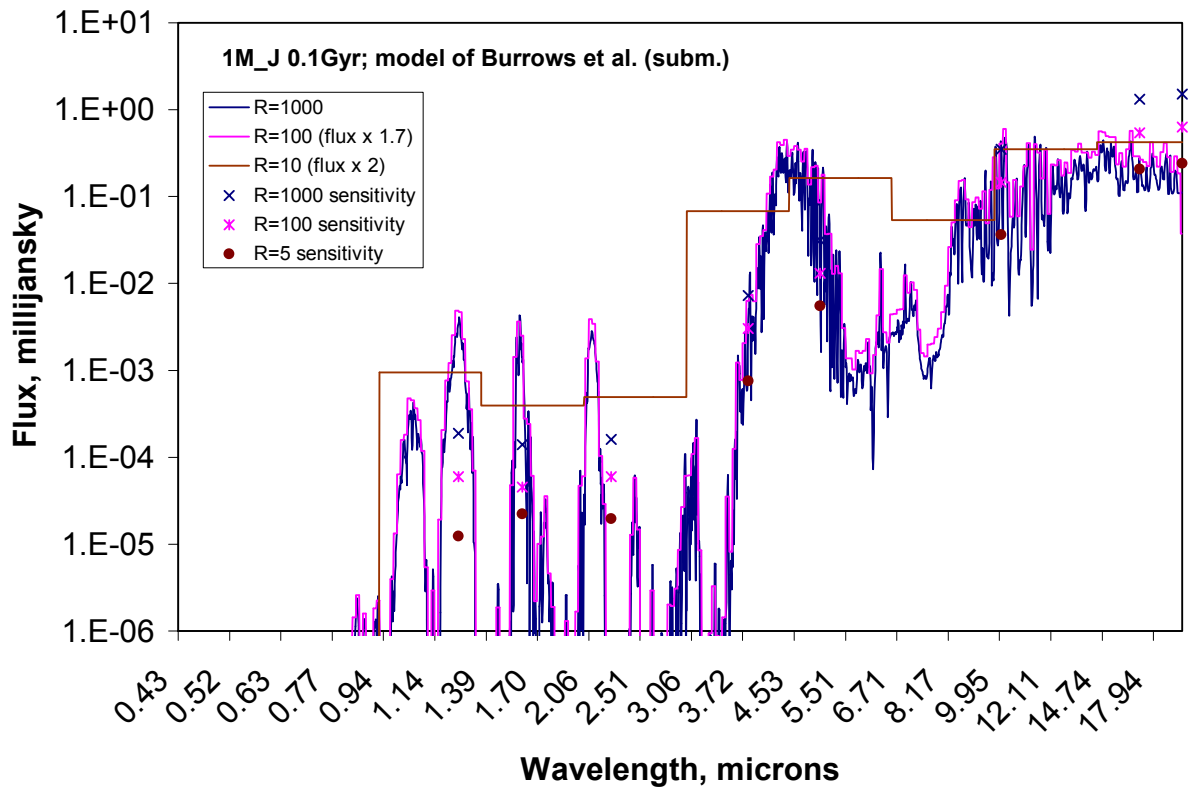


Figure 3. Flux (millijansky) at Earth vs. wavelength (microns) for a one Jupiter mass EGP at  $10^8$  years of age, 10 parsecs distance, isolated. Spectra for  $R = 1000$ ,  $100$ , and  $10$  are shown (the latter two displaced for clarity) along with corresponding GSMT sensitivities, displaced in proportion to the corresponding spectra. GSMT sensitivities, courtesy M. Mountain, are for a  $10^4$  second exposure,  $S/N=10$ , with  $4 \times 4$  pixels across the point source and a GSMT emissivity of 10%.

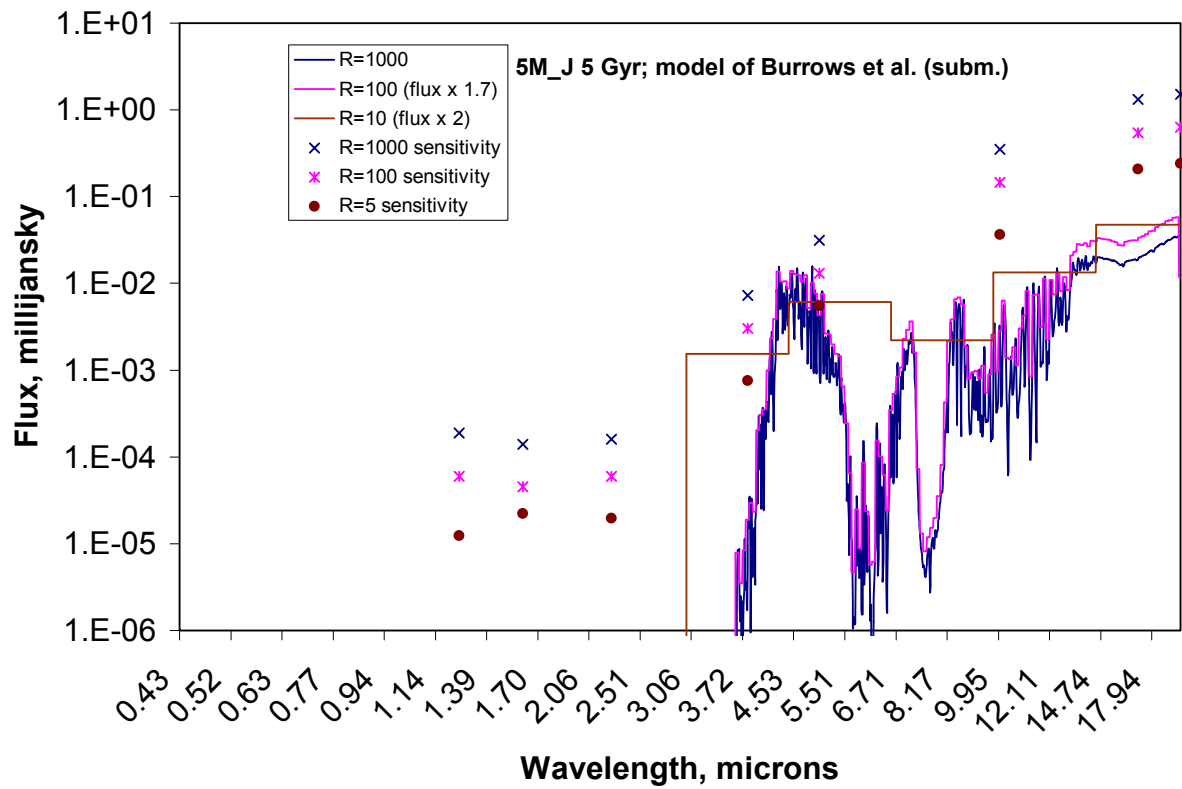


Figure 4. Same as figure 3, for a 5M<sub>J</sub> isolated EGP at 5 x 10<sup>9</sup> years.

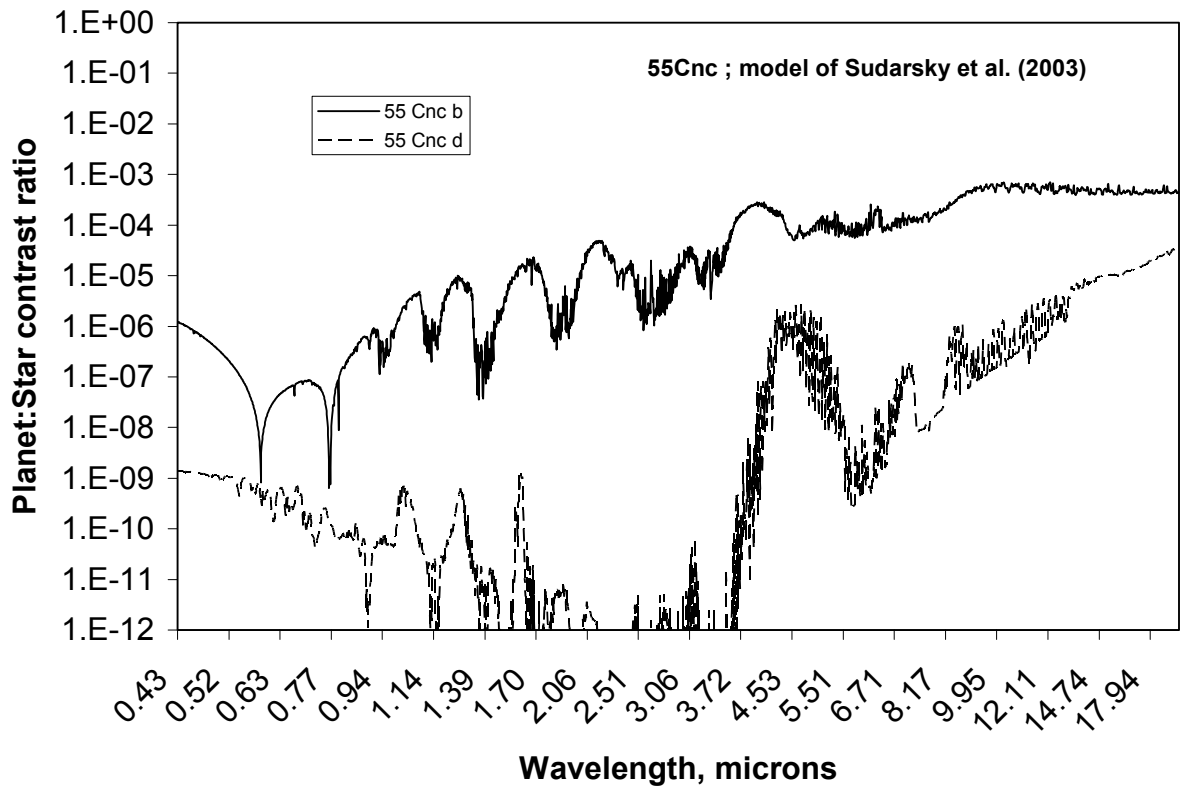


Figure 5. Contrast ratio of the flux from the planet relative to the star for the two EGP's in the system 55 Cnc.

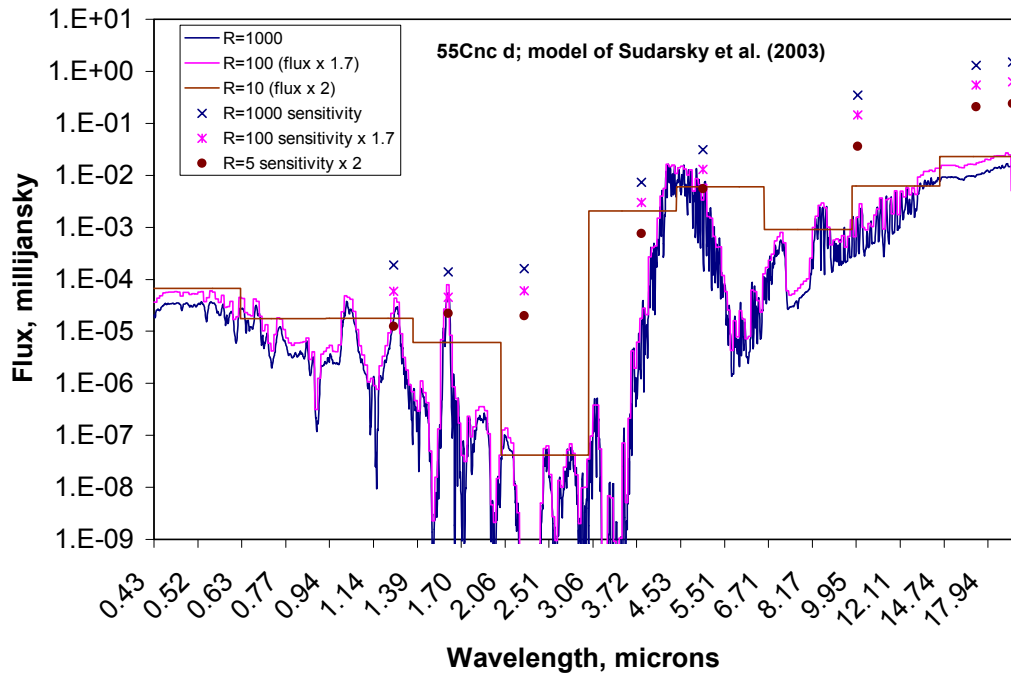


Figure 6. Flux versus wavelength for 55 Cnc d, for three spectral resolutions (displaced from each other for clarity) and corresponding sensitivities. For R=5 the EGP, if separable from the parent star (see figure 5) can be detected with GSMT.

(5) Detectability of Extrasolar Giant Planets: Summary

The models summarized above can be used to predict the limiting distance to which extrasolar giant planets can be detected. Our working assumptions are summarized in Table 1 in which we list the limiting fluxes (nJy) for the indicated wavelengths and spectral resolving powers and a signal/noise ratio of 25 per resolution element.

Table 1: Limiting Fluxes (nJy) to reach S/N =25 in the indicated integration times

$\lambda$ ( $\mu$ )	R=10		R=100		R=1000	
	$10^4$ sec	$10^5$ sec	$10^4$ sec	$10^5$ sec	$10^4$ sec	$10^5$ sec
1.25	8.9 nJy	2.8	42	12	250	67
2.25	38	12	86	27	380	110
3.8	1300	420	4500	1400	18000	5800
4.6	8700	2900	17000	5800	50000	17000

Table 2 lists the planet fluxes estimated from the models described above, while Tables 3 through 6 summarize the limiting distances to which a given planet could be observed by a 30m GSMT.

Table 2: Fluxes (nJ) for Selected Extrasolar Giant Planets

Planet	1.25 $\mu$	2.25 $\mu$	3.8 $\mu$	4.6 $\mu$
1 $M_j$ 100 Myr	3000	2000	8000	$10^5$
2 $M_j$ 100 Myr	$10^5$	$5 \times 10^4$	$10^4$	$3 \times 10^5$
1 $M_j$ 5 Gyr 1.5 AU	6	$10^{-5}$	0.01	1000
1 $M_j$ 5 Gyr 5 AU	69	1	8	$1.1 \times 10^4$

Table 3: Limiting Distances to which a 1 M<sub>j</sub> planet of age 100 Myr can be observed

$\lambda$ ( $\mu$ )	R=10		R=100		R=1000	
	$10^4$ sec	$10^5$ sec	$10^4$ sec	$10^5$ sec	$10^4$ sec	$10^5$ sec
1.25	183pc	327	84	158	35	67
2.25	72	129	48	86	23	43
3.8	24	44	13	24	7	12
4.6	34	58	24	41	14	24

Table 4: Limiting Distances to which a 2 M<sub>j</sub> planet of age 100 Myr can be observed

$\lambda$ ( $\mu$ )	R=10		R=100		R=1000	
	$10^4$ sec	$10^5$ sec	$10^4$ sec	$10^5$ sec	$10^4$ sec	$10^5$ sec
1.25	1060pc	1889	487	912	200	386
2.25	362	645	241	430	115	213
3.8	28	49	15	27	7	13
4.6	58	101	42	72	25	42

Table 5: Limiting Distances to which a 1 M<sub>j</sub> planet located at 1.5 AU of age 5 Gyr can be observed

$\lambda$ ( $\mu$ )	R=10		R=100		R=1000	
	$10^4$ sec	$10^5$ sec	$10^4$ sec	$10^5$ sec	$10^4$ sec	$10^5$ sec
1.25	8 pc	14	3.8	7	1.5	3
2.25	ND	ND	ND	ND	ND	ND
3.8	ND	ND	ND	ND	ND	ND
4.6	3.4	6	2.4	4	1.4	2.4

*Table 6* Limiting Distances to which a 1 M<sub>J</sub> planet located at 5 AU of age 5 Gyr can be observed

$\lambda$ ( $\mu$ )	R=10		R=100		R=1000	
	10 <sup>4</sup> sec	10 <sup>5</sup> sec	10 <sup>4</sup> sec	10 <sup>5</sup> sec	10 <sup>4</sup> sec	10 <sup>5</sup> sec
1.25	27 pc	49	13	24	5.2	10
2.25	1.6	2.9	ND	1.9	ND	ND
3.8	ND	1.4	ND	ND	ND	ND
4.6	11	19	8	14	4.7	8

We conclude that Jovian mass planets of age 100 Myr can be detected and characterized (at R ~ 100) out to the TW Hydra association, provided that they can be separated from their parent star. Detection of ‘old, cold’ Jupiters will be restricted to the immediate solar neighborhood.